

Inhibitory activity of nanoencapsulated quercetin against sodium arsenite-induced sub-acute liver toxicity in rats

Ardhendu Kumar Mandal *^{1,2} , Sibani Sarkar ¹, Aparajita Ghosh ^{1,3} and Nirmalendu Das ^{1,4}

Biomembrane Division¹, Central Instrumentation Division², CSIR-Indian Institute of Chemical Biology, Kolkata, India

Faculty of Paramedical Sciences, Assam down town University, Panikhaiti, Guwahati, India³

Department of Food and Nutrition, Behala College, Parnasree, Kolkata, India⁴

Article Info:



Article History:

Received 26 Aug 2024

Reviewed 03 Oct 2024

Accepted 30 Oct 2024

Published 15 Nov 2024

Cite this article as:

Mandal AK, Sarkar S, Ghosh A, Das N, Inhibitory activity of nanoencapsulated quercetin against sodium arsenite-induced sub-acute liver toxicity in rats, Journal of Drug Delivery and Therapeutics. 2024; 14(11):111-119 DOI: <http://dx.doi.org/10.22270/jddt.v14i11.6835>

*Address for Correspondence:

Ardhendu Kumar Mandal, Central Instrumentation Division, CSIR-Indian Institute of Chemical Biology, 4, Raja S.C. Mullick Road, Jadavpur, Kolkata – 700032, India

Abstract

Arsenic, a metalloid toxicant, is associated with a major global health problem as oxidative stress, a prime cause of tissue toxicity. The subject of our investigation was to assess the therapeutic efficiency of nanoencapsulated quercetin (QC) in combating sodium arsenite (NaAsO₂)-induced sub-acute hepatocellular toxicity in rat model. The rats of the hepatic damage group were injected subcutaneously (s.c.) four dosages of NaAsO₂ (92.36 μM/kg b.wt.) twice a week. The rats of the polylactide nanoencapsulated QC group were injected intravenously (i.v.) four doses of nanoencapsulated QC (8.97 μmol/kg b.wt.) twice a week 2 h after the treatment (s.c.) with 92.36 μM /kg b. wt. NaAsO₂ twice a week for four doses. The rats of the empty nanocapsule or free QC treated group were injected i.v. four doses empty nanocapsule or free QC twice a week 2 h after the treatment (s.c.) with same doses of NaAsO₂ twice a week for four doses. Arsenic deposition (580±20 μg/g protein) observed in liver tissue of rats treated with arsenite (92.36 μM/kg b.wt.), was found to reduce (120±9 μg/g protein) by the treatment of nanoencapsulated QC in rats significantly ($p<0.001$). The levels of antioxidant enzymes and GSSG/GSH ratio enhanced ($p<0.001/0.1/0.01$) by the treatment of NaAsO₂ were reduced by the post treatment of nanoencapsulated QC significantly ($p<0.001/0.01$). The levels of ROS, lipohydroperoxide or membrane microviscosity increased or decreased ($p<0.001$) by the treatment of NaAsO₂ were monitored to reduce or enhance significantly ($p<0.001$) by the treatment of nanoencapsulated QC in rat liver respectively. The blood serum biochemical levels enhanced ($p<0.001$) by the treatment of NaAsO₂ were found to reduce significantly ($p<0.001$) by the treatment of nanoencapsulated QC in rats. The TGFβ1 and MMP-13 in the rat plasma augmented ($p<0.001$) by the treatment of NaAsO₂-exposure were found to decline ($p<0.001$) significantly by the treatment of nanoencapsulated QC in rats. The rats in the other groups such as empty nanocapsule or free QC treated showed no or less inhibitory efficiency against NaAsO₂-treatment compared to nanoencapsulated QC treated group. Application of nanoencapsulated QC may be a potent formulation to get higher inhibitory therapeutic efficiency against NaAsO₂-induced sub-acute hepatocellular toxicity.

Keywords: Arsenic; Sub-acute hepatocellular toxicity; Oxidative stress; Nanoencapsulated QC; Inhibitory therapeutic efficiency

INTRODUCTION

Arsenic, a metalloid environmental toxicant, widely investigated in both inorganic and organic forms in the crust of the earth, contaminated diet (sea food, meats and grains), air, ground or surface water, may cause a variety of global human health disorders ¹⁻¹⁰. Arsenics prevalent in the environment as trivalent arsenite and pentavalent arsenate forms, while arsenite is considered as more toxic than arsenate owing to their capability to anchor with the sulphydryl protein to disorganize the enzyme activity ¹¹. The maximum contaminant level for arsenic exposure has been evaluated 10 ppb (10 μg/l) by the World Health Organization (WHO) and the U.S. Environmental Protection Agency (EPA) in 2016 ⁴. The metabolism of arsenic exerts its toxicity through the inhibition of the activities of around 200 enzymes

correlated to the cellular energy pathways, DNA synthesis and repair ^{12,13}. Trivalent arsenics may be contiguously methylated to volatile product/s, while their pentavalent forms are not promptly picked up by cells, but are reduced to their trivalent forms ¹⁴. The arsenics are metabolized mainly in the liver after their administrations, while hepatocytes capture trivalent arsenics followed by their subsequent conjugations and methylations resulting in volatile products ¹⁵. In general, arsenics are metabolized by the reductions and methylation reactions catalyzed by the glutathione-S-transferase omega-1s (GSTO1s) and arsenic (III) methyltransferases (AS3MTs) engaging arsenic methylations through one-carbon metabolisms by S-adenosyl methionines (SAMs) as methyl donors and to require reduced glutathiones (GSHs) as electron donors

in reductase reactions, while GSTO1s reduce methylarsenates [MA(V)s] and arsenates [As(V)s] to methylarsonites [MA(III)s] and arsenites [As(III)s], respectively, and the toxic trivalent arsenicals produced during reductions are detoxified by AS3MTs to less toxic pentavalent arsenicals such as methylarsonates [MA(V)s] and dimethylarsenates [DMA(V)s]¹⁶.

Arsenic causes hepatocellular disorders mainly through the induction of hepatic cellular injury by the productions of reactive oxygen species (ROS) (superoxide, O_2^- , peroxy, $ROO\cdot$ radicals hydroxyl, $\cdot OH$, and hydrogen peroxide, H_2O_2), owing to the imbalance between pro-oxidant and antioxidant homeostasis, and the fascination of binding to sulfhydryl proteins and thiols of GSH¹⁷. ROS produced by the metabolic intermediates of arsenics through the induction of CYP450 families or activated inflammatory cells via NADPH oxidases promote lipid peroxidation products to cause liver injury¹⁸. The elevated ROS can overpower the antioxidant defense system to create oxidative damages of cellular components such as proteins, lipids, and DNA leading to impairment of cellular function as well as alterative expressions of proteins or genes¹⁹⁻²¹.

As enhanced generation of ROS because of the arsenics-induction directs to rapid consumptions and depletions of endogenous free radical scavenging antioxidants, it is required to incorporate exogenous antioxidants as therapeutics to counter the oxidative stress for the inhibition of oxidative injury²².

Quercetin, a known polyphenolic flavonoidal free radical scavenging antioxidant, generally existed in huge amounts in vegetables, tea, fruits, red wine, and olive oil, may be utilized as exogenous drug to treat against oxidative stress-induced injury or damage²³. However, simple antioxidant treatment is not a believing perspective to counteract the oxidative damages for its poor bioavailability to deal with hepatocellular membranes²⁴. Therefore, it is indeed to develop a delivery system to vector an elevated pool of antioxidants to the targeted cells^{25,26}. Nanocapsule has been accepted as a potential drug delivery vehicle for its nontoxic, biodegradable, non-immunogenic, site-specific and controlled drug-liberating capability in the biological systems²⁷.

The objectives of our studies were to optimize the dose of flavonoidal quercetin into the polylactide nanocapsule formulation and to investigate its biological therapeutic efficacies against arsenite-induced sub-acute hepatocellular oxidative damages as well as upregulated biomarker levels in rat livers.

MATERIALS AND METHODS

Materials

Poly-D-L-lactide (PLA), phosphatidyl ethanolamine (PE), dichloromethane, isopropyl myristate, xanthine, ferricytochrome-c, xanthine oxidase, tween-80, and urethane were purchased from Sigma chemicals (St. Louis, MO, USA). QC was secluded from Buck wheat (*Fagopyrum esculentum*). All other purchased reagents were of analytical grades.

Methods

Preparation of quercetin-loaded nanocapsules

Briefly, 35 mg PLA was dissolved in 20 mL of dichloromethane (DCM). 50 mg phosphatidyl ethanolamine was dissolved in 500 μL of isopropylmyristate along with QC (9 mg), and the solution is mixed with DCM mixture. The organic suspension was allowed to run gently into 100 mL of 0.025M phosphate buffer saline (PBS) (pH 7.2) bearing 0.4% Tween 80 (the non-ionic surfactant) under modest magnetic stirring for 3 h, and, any remnants left, were removed by passing the nitrogen gas for 5-10 mins. The suspension was spun at 35,000 rpm (105,000g) in Sorval RC 5B Plus utilizing the rotor Sorval T-865 for 1h. The pellets of nanocapsules were cleansed with PBS followed by collection and re-suspension in 4 mL of PBS.

For estimating the intercalated nanocapsules, the deposits were dissolved in 4 mL of DCM, and retain for 3 days at 4°C. The O.D. was determined at 369 nm λ_{max} . The total amount of QC ($\epsilon_m = 0.038251 \text{ mol}^{-1}\text{cm}^{-1}$) in the nanocapsule-form was estimated from the QC-concentration in the dissolved deposit divided by the total amount of drug adjoined during the preparation of nanocapsule. The percentage of incorporation of QC in the nanocapsule was estimated to 45% of the added amount.

Animals and treatments

Male Sprague Dawley rats, each weighing 100-130 g were acclimatized to a laboratory conditions (26-28°C, 60-80% relative humidity, 12h dark/light cycle) for 7 days prior to the onset of the treatment through which they obtained arsenic free food (commercially pelleted rat chows, bought from Hindustan Unilever Limited, Maharashtra, India) and drinking waters ad libitum. Rats were haphazardly chosen for groups and arsenic, drug or nanocapsules (free or loaded) were administered according to individual's body weight. Rats were separated into six groups containing five rats in each group. Rats of the normal group (A) were injected s.c. 4 doses of physiological saline (5 mL/kg b.wt.) twice a week. Rats in the (A) + nanoencapsulated QC treated group were injected i.v. 4 doses of nanoencapsulated QC (8.97 μmol / kg b. wt.) suspension (5 mL/kg b. wt.) 2 h after administration (s.c.) of physiological saline twice a week. Rats in the sodium arsenite treated group (B) were injected s.c. 4 doses of sodium arsenite (92.36 μM /kg b. wt.) suspension (5 mL/kg b. wt.) twice a week. Rats in (B) + empty nanocapsule treated group, (B) + free QC treated group, and (B) + nanoencapsulated QC treated group were injected i.v. 4 doses of empty nanocapsule (5 mL/kg b. wt. suspension), free QC (8.97 μmol /kg b. wt. in suspension (5 mL/kg b. wt.), or nanoencapsulated QC (8.97 μmol /kg b. wt.) suspension (5 mL/kg b. wt.) twice a week 2 h after administration (s.c.) of 4 doses of sodium arsenite (92.36 μM /kg b. wt.) suspension (5 mL/kg b. wt.) twice a week, respectively. All the animals utilized in this investigation obtained proper care and handling in compliance with Animal Ethics Committee, India, Registration No. 147/99/CPC SEA. All animal

experiments were conducted following the guideline of the "Principles of laboratory animal care" (NIH publication number 85-23, 1985) and only after receiving the approval of the Institutional Animal Ethics Committee.

General procedures

After 14 days of treatments, rats of all treated groups were anaesthetized by a single intraperitoneal (i.p.) injection of urethane (35 mg/kg) and blood was gathered by cardiac puncture ²⁸. One blood part was retained to prepare plasma, and the other for serum. To prepare serum, blood was spun at 2000xg for 10 min at 4°C for assaying the activities of serum enzymes. Plasma was prepared by the addition of the anticoagulant heparin followed by spinning. Serum alkaline phosphatase (AP) and serum aspartate transaminase (AST) ^{29,30} and serum urea and creatinine (modified Berthelot and alkaline picrate methods) were estimated utilizing the standard kits manufactured by Coral clinical systems, India. The plasma was utilized for TGF- β and MMP-13 measurements. After collections of blood, all animals were decapitated followed by quick isolations of their livers and cleansing with cold physiological saline. One part of the liver was used for few experiments, and the other parts were stored at -80°C for further experiments.

Activities of antioxidant enzymes

After homogenizing a portion of the liver in 0.25M sucrose solution, the homogenate was spun at 8200xg for 10 min utilizing a Sorvall SS34 rotor. The obtained supernatant was centrifuged at 105,000xg for 1 h in an OTD-50B Sorvall ultracentrifuge (4°C). The supernatant obtained from the 2nd spinning was collected as the cytosolic fractions of the liver.

The assay of superoxide dismutase (SOD) (EC1.15.1.1) in liver cytosolic fraction was estimated by following the methodology utilizing spectrophotometer with a few modifications ³¹. The SOD activity was expressed in unit by assuming the enzyme activity as one unit that inhibited the initial reduction rate of ferricytochrome c (10 mM) by 50% determined using Rayleigh UV 2601 double beam spectrophotometer ³².

A part of the cytosolic fraction was utilized to estimate catalase activity ³³. The reaction mixture comprised 50 μ L of enzyme extract, sodium phosphate buffer (0.05 M, pH 7.0), and 50 mM⁻¹ H₂O₂ in a 3 mL volume. The enzyme activity was determined by monitoring the reduction in absorbance at 240 nm as a resultant of consumption of H₂O₂, and expressed as amount of H₂O₂ decomposed/min/mg protein.

Glutathione peroxidase (GPx) activity from liver cytosolic fraction was determined ³⁴. The cytosol containing enzymes was admixed with 0.25 M potassium phosphate buffer, 20 mM NADPH, 25 mM EDTA, 40 mM glutathione (GSH), and glutathione reductase (GR). The enzyme activity was assayed and expressed as μ mol NADPH oxidized/min/mg protein.

The cytosolic glutathione reductase (GR) was estimated following the method ³⁵. A 3 mL mixture contained 25-

50 μ L of enzyme extract, 100 mM phosphate buffer (pH 7), 0.1 mM NADPH, 1mM EDTA, and 1 mM GSSG. The rate of NADPH oxidation was evaluated by monitoring the reduction in absorbance at 340 nm with a spectrophotometer. The enzyme activity was expressed as μ mol of NADPH oxidation/min/mg protein.

The cytosolic glutathione-S-transferase (GST) activity was estimated spectrophotometrically utilizing 1-chloro-2,4-dinitrobenzene (CDNB) ³⁶. The formation rate of CDNB-GSH complex was noticed at 340 nm, and utilized for expressing the enzyme activity.

The cytosolic glucose-6-phosphate dehydrogenase (G6PDH) activity was measured utilizing a Sigma Diagnostics kit with slight modifications ³⁶. The formation rate of NADPH is proportional to the G6PDH activity estimated spectrophotometrically as an enhancement of absorbance at 340 nm. One unit of G6PDH activity was expressed as 1 μ M NADPH produced/min.

Estimation of reduced glutathione (GSH) level

Glutathione level of liver homogenate was estimated with the support of a spectrophotometer utilizing tetrachloro-acetic acid with EDTA as a protein precipitating reagent ³⁷. The mixture was incubated for 5 min prior to the spinning for 10 min at 200xg at 4°C. The mixture was then transferred to other tubes, and Ellmen reagent (5, 5' dithiobis-2 nitrobenzoic acid in 1% sodium citrate) and 0.3 M phosphate buffer were adjoined. After the accomplishment of the total reaction, the solutions were read at 412 nm, while the absorbance values were contrasted with a standard curve produced from the familiar GSH concentration for evaluating the GSH levels of liver homogenate.

Estimation of total arsenic contents

Arsenic administered s.c. to the rats and for the treated groups was estimated after 14 days of treatments. In brief, liver homogenates were digested with the mixture of acids (nitric acid:sulfuric acid:perchloric acid, 6:1:1) over a controlled heater. After digestion, the acid mixture was evaporated out with the adding up of triple distilled water, and the obtained solution was exploited for the determination of arsenic contents through flow injection utilizing atomic absorption spectrophotometer (Spectra AA 30/40; Varian, Inc., Palo Alto, CA).

Estimation of ROS level

Intracellular ROS level was estimated in liver tissue ³⁸. In brief, the homogenized (10% in PBS, pH 7.2) hepatic cells (0.4 mg/mL) were added to the cell permeant probe CM-H₂DCFDA (5-(and-6)-chloromethyl-2', 7'-dichlorodihydro-fluorescein diacetate acetyl ester) (2 μ M) for 15 min at 30°C to monitor the fluorescence of generated dichlorofluorescein compound through the oxidation of H₂DCF by hydroxyl radicals (OH), hydrogen peroxides (H₂O₂) or other peroxides generated in the cells, relating the fluorescence intensities, proportional to the amounts of ROS generated. Fluorescence was determined utilizing spectrofluorometer (LS 3B, Perkin Elmer, USA) as excitation at 499 nm and emission at 520

nm wavelengths, and explicated as relative fluorescence intensities considering the values of normal as 100%.

Estimation of lipid peroxidation

Lipid peroxidations in the liver membranes were estimated through the measurements of the amounts of conjugated dienes utilizing a spectrophotometer³⁹. Lipids, extracted from the liver homogenates in a chloroform-methanol mixture (2:1, v/v), were evaporated to dryness under nitrogen atmosphere at 25°C, and redissolved in n-cyclohexane for assaying at 234 nm. The results were revealed as μ mol of lipohydroperoxide/mg protein by utilizing ϵ_m of $2.52 \times 10^4 M^{-1} cm^{-1}$. Total proteins were estimated following the methodology⁴⁰.

Fluorescence depolarization estimation of the fluidity of liver cell membranes

The fluorescence depolarizations, linked to the hydrophobic fluorescence probes diphenyl hexatrienes (DPHs), were measured in the liver cell membranes by using spectrofluorimeter to observe the alterations in the fluidity of the lipid matrixes accompanying to gel to liquid crystalline phase transitions³⁷. The plasma membrane fractions of liver cells were incubated at 37°C with the adjoining of DPHs dissolved in tetrahydrofurans (DPH/lipid molar ratio 1:500). The emission and the excitation maxima were kept at 430 nm, and 365 nm respectively. The fluorescence anisotropy was determined by utilizing the equation, $r = (I_{\parallel} - I_{\perp}) / (I_{\parallel} + 2I_{\perp})$, where I_{\parallel} and I_{\perp} are the fluorescence intensities in parallels and perpendiculars to the directions of polarizations of the excited lights. The

microviscosity parameters $[(r_0/r) - 1]^{-1}$ were determined in every cases, understanding the maximum limiting fluorescence anisotropies (r_0), which for DPHs are 0.362⁴¹.

Estimation of plasma transforming growth factor beta 1 (TGF- β 1) and matrix metallo proteinase-13 (MMP-13) levels

Plasma TGF- β 1 and MMP-13 levels were estimated utilizing ELISA kits (R&D Systems, Catalog MB 100B, and Abbexa, Catalog ABX 155829, respectively).

Statistical analysis

Statistical analysis was accomplished with one-way ANOVA with post hoc Tukey's test. The software utilized was version 15.0; SPSS Inc: Chicago, IL. In all cases, $P < 0.05$ was intended as the minimal level of significance.

RESULTS

Effect of QC in nanocapsules on $NaAsO_2$ -induced antioxidant enzymes

Normal rats, injected with nanoencapsulated QC, exhibited a slight enhancement of different antioxidant enzyme activities in hepatic cells. The subcutaneous administration of $NaAsO_2$ (92.36 μ M/kg b. wt, 4 dosages, twice a week) showed a marked decrease of those enzyme levels. Empty nanocapsules or free QC groups provided no or less significant inhibition from arsenic insults, while nanoencapsulated QC treatment inhibited the decrement of enzyme activities maximally in hepatic cells (Table 1).

Table 1: Effect of quercetin in free and nanoencapsulated forms on the changes in SOD, catalase, GPx, GR, GST and G6PDH activities in rat liver by the exposure of sodium arsenite.

Groups	SOD (U/mg protein)	Catalase (μ mol H_2O_2 reduced/min/mg protein)	GPx (μ mol NADPH oxidation/min/mg protein)	GR (μ mol NADPH oxidation/min/mg protein)	GST (nmol produced/min/mg protein)	G6PDH (nmol NADP reduced/min/mg protein)
Normal (A)	64.48 \pm 2.04	6.86 \pm 0.42	9.26 \pm 1.44	30.68 \pm 1.68	105.56 \pm 1.62	11.69 \pm 1.67
(A)+Nanoencapsulated QC treated	68.86 \pm 2.48	7.98 \pm 0.46	10.47 \pm 1.47	32.14 \pm 1.92	108.73 \pm 1.98	13.83 \pm 1.98
Sodium arsenite treated (B)	18.98 \pm 0.74 ^c	2.69 \pm 0.11 ^c	3.69 \pm 0.12 ^a	9.78 \pm 0.62 ^c	48.96 \pm 0.48 ^c	3.27 \pm 0.24 ^b
(B)+Empty nanocapsule treated	21.67 \pm 0.85	2.86 \pm 0.15	4.48 \pm 0.16	12.04 \pm 0.81	51.89 \pm 0.62	4.64 \pm 0.32
(B)+Free QC treated	27.12 \pm 1.10	4.60 \pm 0.24	6.11 \pm 0.46	16.15 \pm 1.12	60.41 \pm 0.74	7.13 \pm 0.75
(B)+Nanoencapsulated QC treated	56.88 \pm 1.78 ^e	6.18 \pm 0.39 ^e	8.67 \pm 0.91 ^d	27.86 \pm 1.42 ^e	92.88 \pm 1.36 ^e	10.87 \pm 1.38 ^d

Results are expressed as mean \pm S.E. of five rats. ^{a/b/c}P<0.1/0.01/0.001, significantly different from normal. ^{d/e}P<0.01/0.001, significantly different from sodium arsenite treated (B).

Effect of nanoencapsulated QC on $NaAsO_2$ -induced GSSG/GSH ratio levels in the rat-hepatic tissue

The GSSG/GSH ratio, the marker of oxidative stress, was slightly reduced in normal rats treated with nanoencapsulated QC, in comparison to normal rats. The four doses (twice a week) of $NaAsO_2$ administration

(92.36 μ M/kg b. wt.) induced marked enhancement in this ratio. However, no or less significant decrement of the ratio was noticed in the rats treated with empty nanocapsules or free QC, while the maximal decrement was monitored in the rats treated with nanoencapsulated QC (Figure 1).

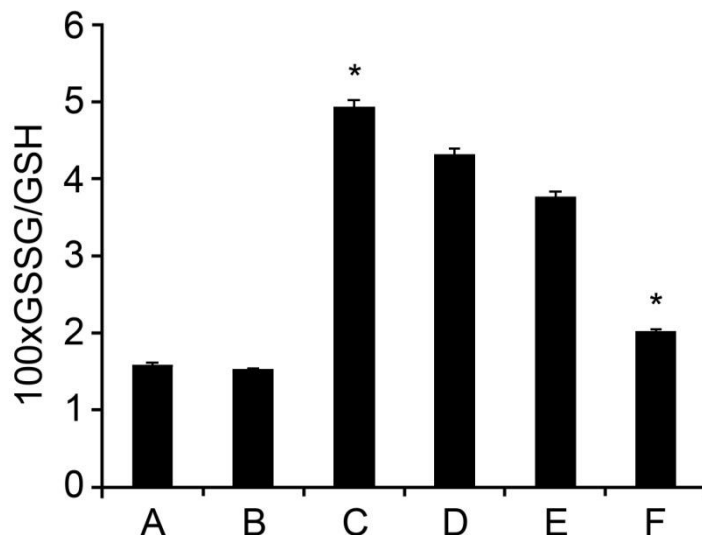


Figure 1: Values of GSSG/GSH ratio in hepatic tissue from normal, sodium arsenite and nanoencapsulated QC treated rats. The groups are normal (A), A+ Nanoencapsulated QC treated (B), Sodium arsenite treated (C), C + Empty nanocapsule treated (D), C + Free QC treated (E), and C + Nanoencapsulated QC treated (F). Values are mean \pm S.E. of 5 rats. *P<0.001 (C) significantly different from normal. *P<0.001 (F) significantly different from arsenite treated rats.

Effect of nanoencapsulated QC on NaAsO₂-induced uptake of inorganic arsenic in rat liver

The four doses (twice a week) of NaAsO₂ (92.36 μ M/kg b. wt.) induced the marked amount of accumulation of arsenics in hepatic cells. No or less significant inhibitions were noticed in rats exposed with empty

nanocapsules or free QC, 14 days after arsenic exposure. The maximal decrement was noticed by nanoencapsulated QC administration. No detectable amount of arsenic was traced in the liver-homogenate of normal and nanoencapsulated QC treated rats, received no arsenic in food and drinking water (Figure 2).

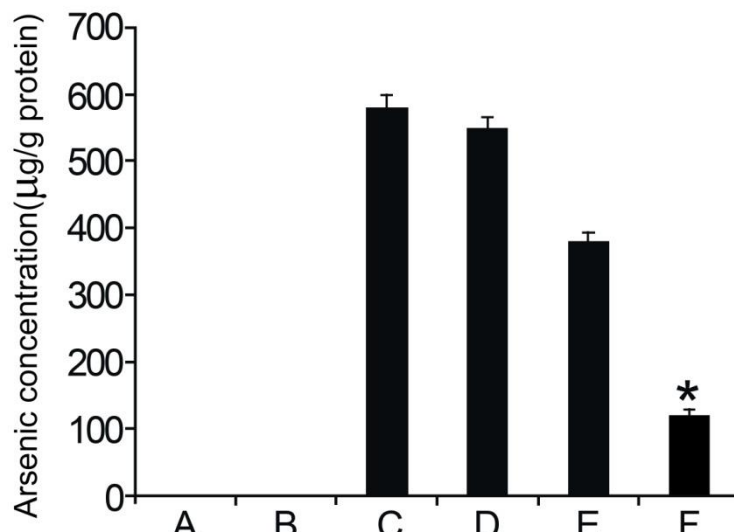


Figure 2: Values of arsenic levels in hepatic tissue from normal, sodium arsenite and nanoencapsulated QC treated rats. The groups are normal (A), A+ Nanoencapsulated QC treated (B), Sodium arsenite treated (C), C + Empty nanocapsule treated (D), C + Free QC treated (E), and C + Nanoencapsulated QC treated (F). Values are mean \pm S.E. of 5 rats. *P<0.001 (F) significantly different from arsenite treated rats.

Effect of nanoencapsulated QC on NaAsO₂-induced ROS, lipid peroxidation and membrane microviscosity in rat-liver tissue

Normal rats treated with nanoencapsulated QC exhibited almost similar values in ROS production, conjugated diene levels, or microviscosity level, respectively, compared to normal rats. The administration of four dosages (twice a week) of NaAsO₂ (92.36 μ M/kg b. wt.) induced a remarkable increase, or decrease, respectively in those levels. No or less

significant decrement, or enhancement in ROS, diene levels, or microviscosity level were noticed respectively in the rats treated with empty nanocapsules or free QC, 14 days after arsenic administration. The maximal decrement or increment of the ROS, conjugated diene levels, or microviscosity level was noticed in the rats exposed with nanoencapsulated QC (Table 2).

Table 2. Effect of quercetin in free and nanoencapsulated forms on the changes in the generation of reactive oxygen species (ROS) i.e. DCF fluorescence, lipid peroxidation levels (lipohydroperoxide) and membrane microviscosity in rat livers by the administration of sodium arsenite.

Groups	DCF-fluorescence (% of normal)	Lipohydroperoxide ($\mu\text{mol}/\text{mg protein}$)	Membrane microviscosity [$r_0/r-1]^{-1}$
Normal (A)	100 \pm 5.86	1.38 \pm 0.03	1.32 \pm 0.15
(A)+Nanoencapsulated QC treated	98 \pm 4.24	1.32 \pm 0.02	1.45 \pm 0.16
Sodium arsenite treated (B)	278 \pm 12.25*	7.14 \pm 0.08*	0.43 \pm 0.05*
(B)+Empty nanocapsule treated	270 \pm 11.47	6.48 \pm 0.07	0.49 \pm 0.06
(B)+Free QC treated	240 \pm 9.56	5.45 \pm 0.06	0.72 \pm 0.08
(B)+Nanoencapsulated QC treated	117 \pm 7.23#	1.91 \pm 0.04#	1.05 \pm 0.12#

Values are mean \pm S.E. of five rats. *P< 0.001 significantly different from normal. #P< 0.001 significantly different from sodium arsenite treated (B) rats.

Effect of nanoencapsulated QC on NaAsO₂-induced upregulation of TGF- β and MMP-13 levels in rat blood plasma

Normal rats treated with nanoencapsulated QC, showed almost similar concentrations in TGF- β or MMP-13 level compared to normal rats. The four dosages (twice a week) of NaAsO₂ (92.36 $\mu\text{M}/\text{kg}$ b. wt.) induced a marked increment of TGF- β or MMP-13 concentration in blood plasma compared to normal rats. Empty nanocapsules or free QC treatment provided no or less significant alteration in TGF- β or MMP-13 level in blood plasma, while nanoencapsulated QC treatment showed a marked decrement in TGF- β or MMP-13 level in blood plasma of NaAsO₂-treated rats (Figures 3 and 4).

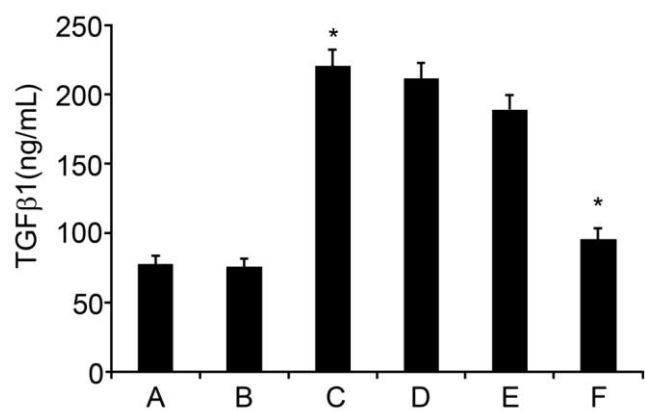


Figure 3. Effect of nanoencapsulated QC treatment on TGF- β 1 concentration in rat plasma. The groups are normal (A), A+ Nanoencapsulated QC treated (B), Sodium arsenite treated (C), C + Empty nanocapsule treated (D), C + Free QC treated (E), and C + Nanoencapsulated QC treated (F). Values are mean \pm S.E. of 5 rats. *P<0.001 (C) significantly different from normal. *P<0.001 (F) significantly different from arsenite treated rats.

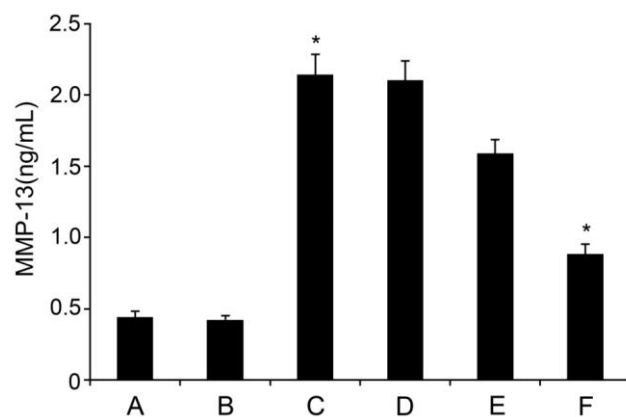


Figure 4: Effect of nanoencapsulated QC treatment on MMP-13 concentration in rat plasma. The groups are normal (A), A+ Nanoencapsulated QC treated (B), Sodium arsenite treated (C), C + Empty nanocapsule treated (D), C + Free QC treated (E), and C + Nanoencapsulated QC treated (F). Values are mean \pm S.E. of 5 rats. *P<0.001 (C) significantly different from normal. *P<0.001 (F) significantly different from arsenite treated rats.

Effect of QC-loaded nanocapsules on NaAsO₂-induced hepatocellular and nephro toxicity

Normal rats administered with nanoencapsulated QC exhibited almost similar results with the normal rats. Rats injected with four doses (twice a week) of NaAsO₂ (92.36 $\mu\text{M}/\text{kg}$ b. wt.) provided significantly developed liver and renal toxicity noticed from enhanced AP, AST and creatinine, urea values in serum. Empty nanocapsules or free QC treated group exerted no or less significant inhibition against NaAsO₂-induced hepatic and renal toxicity. The degree of inhibited values was monitored maximally in liver and nephro toxicity by the nanoencapsulated QC treatment exposed with arsenic (Table 3).

Table 3: Effect of nanoencapsulated quercetin on blood serum biochemical parameters in sub-acute sodium arsenite-induced hepatocellular damages.

Groups	AP (U/L)	AST (IU/L)	Urea (g/L)	Creatinine (mg/L)
Normal (A)	265±9.23	30.36±1.46	0.43±0.04	12.47±1.56
(A)+Nanoencapsulated QC treated	263±8.76	27.89±1.33	0.41±0.03	11.58±1.42
Sodium arsenite treated (B)	794±23.18*	118.24±7.02*	1.53±0.08*	58.26±6.14*
(B)+Empty nanocapsule treated	772±17.34	114.57±6.12	1.46±0.07	55.62±5.02
(B)+Free QC treated	728±13.67	100.14±5.56	1.28±0.06	45.26±4.32
(B)+Nanoencapsulated QC treated	296±10.49#	45.28±3.12#	0.54±0.05#	17.86±2.38#

Results are expressed as mean ± S.E. of five rats. *P<0.001, significantly different from normal. #P<0.001, significantly different from sodium arsenite treated (B).

DISCUSSION

In biological system, arsenite initiates generation of toxic ROS such as O_2^- , $\cdot OH$ and H_2O_2 which cause oxidative damage through lipid peroxidation, thiol depletion, and up-regulations of biomarkers evidenced by our results ²⁰ (Tables 1-3, Figures 1-4). ROS interact with cellular components such as protein, lipid, thiols, carbohydrate, DNA, and other low molecular weight antioxidants, and cause oxidation of macro molecules, resulting in pathophysiological outcomes.

Several drugs such as arsenic specific antidotes have been applied to diminish liver damage. However, they are not cell type specific or liver specific ⁴². QC, a polyphenolic flavonoid, is familiar to diminish toxicant-induced hepatic damage ⁴³. Nanoencapsulated QC has been formulated by us for its targeted delivery to hepatocytes at a high uptake rate and tested in diminishing $NaAsO_2$ -induced hepatocellular damage. We have noticed that nanoencapsulated QC interacts with targeted cells at a faster rate compared to free QC. As clinical trial of this flavonoid against toxicant-induced tissue injury is not possible owing to its insoluble nature, vesicular QC as drug delivery system may be a suitable formulation to check toxicant-induced cellular damage.

Previous studies have exhibited the deviations of the pro-oxidant/antioxidant balances in arsenite-exposed rats with the decrement of antioxidant levels and the subsequent development of oxidative damage ⁴⁴. Our investigations have indicated that the hepatic injury is correlated with the uptake of arsenic, the enhancement of GSSG/GSH ratio and the impaired activity or demolition of hepatocellular antioxidant level in $NaAsO_2$ -treated rats. Maximal decrement of liver damage as well as the enhancement of antioxidant level and the reduction in GSSG/GSH ratio accompanied with marked demolition of arsenic contents in liver cells were observed by the nanoencapsulated QC treatment in comparison to empty nanocapsules or free QC treatments (Table 1, Figures 1 and 2). The mechanisms of the inhibitory effects of nanoencapsulated QC against arsenite-induced hepatic injury may be linked primarily to the depletion of arsenic accumulation in hepatic cells

possibly owing to the arsenic chelation and / or inhibition of hepatic arsenic entry ⁴⁵.

It may be postulated that the enhanced arsenic deposition in liver tissue from $NaAsO_2$ -exposed rats produced maximum ROS and subsequent lipohydroperoxides accompanied with the maximum reduction in membrane microviscosity. The maximal reduction of hepatocellular generation of ROS and lipohydroperoxides, and maximal enhancement of membrane microviscosity level were occurred by the nanoencapsulated QC treatment when the arsenic accumulation in hepatic cells was maximally restricted correlating the inhibitory activity of QC against arsenite-induced cell damage (Table 2).

Fibrogenesis is initiated in the liver through the induction of oxidative stress by the exposure of toxicant, while the biomarkers such as TGF- β and MMP-13 may take key roles in the development of fibrosis and extracellular matrix remodeling ⁴⁶. Our investigations denote that arsenite induced the up-regulations of TGF- β 1 and MMP-13 in rat plasma, while nanoencapsulated QC treatment inhibited maximally the up-regulations correlating the inhibitory role of targeted delivery of QC in liver through the inactivation of MMP-13-induced TGF- β 1 synthesis (Figures 3 and 4).

The levels of AP, AST and urea, creatinine in blood serum were found increased by the treatments of $NaAsO_2$. The targeted delivery of nanoencapsulated QC inhibited maximally $NaAsO_2$ -induced hepatocellular membrane damages through checking their leakages in the blood circulation compared to empty nanocapsules or free QC treatments (Table 3).

As the biodegradable and biocompatible polymeric nanocapsules have longer blood circulation time with no degradation by circulating lipases and preventing capability of the drug from biological environment, they may take pivotal role in targeted delivery of QC to liver owing to their common colloidal particles clearance characteristics from circulation by liver. Therefore, QC in nanoencapsulated form may be considered as targeted delivery device that sustained the drug release vehicle to reduce the overall hepatic toxicity through their biological efficiency by free radical scavenging

activity in combating arsenite-induced oxidative liver damage.

CONCLUSION

Our approach to deliver a nontoxic biodegradable herbal polyphenolic flavonoid QC selectively to liver might have a therapeutic potency for inhibiting NaAsO₂-induced sub-acute hepatic toxicity. The usages of polylactide nanoencapsulated QC formulated with a very low dosage of the drug components may be considered as a potential therapeutic perspective for arsenite-induced liver toxicity/disorder through a substantial inhibition of hepatic damage against arsenite-intervened oxidative stress.

Acknowledgements and Financial and competing interest disclosure

This study was supported financially by Council of Scientific and Industrial Research (CSIR), Govt. of India, New Delhi and Supra Institutional Project, Indian Institute of Chemical Biology, Kolkata Project number SIP 0007. The authors have no other relevant affiliations or financial involvement with any organization or entity with a financial interest in or financial conflict with the subject matter or materials discussed in the manuscript apart from those disclosed.

No writing assistance was used in the production of this manuscript.

Ethical conduct of research

The authors state that they have obtained appropriate institutional review board approval or have followed the principles outlined in the Declaration of Helsinki for all human or animal experimental investigations.

Author contributions

Conceived and designed the experiments: AKM, ND. Performed the experiments: AKM. Analyzed the data: AKM. Contributed materials/reagents/analysis tools: AKM, SS, AG. Wrote the manuscript: AKM. Edited the manuscript: ND.

Source of Support: Nil

Data Availability Statement: The data presented in this study are available on request from the corresponding author.

REFERENCES

- Argos M, Kalra T, Rathouz PJ, Chen Y, Pierce B, Parvez F, et al. Arsenic exposure from drinking water, and all-cause and chronic disease mortalities in Bangladesh (HEALS): A prospective cohort study. *Lancet.* 2010; 376(9737):252-58. [https://doi.org/10.1016/S0140-6736\(10\)60481-3](https://doi.org/10.1016/S0140-6736(10)60481-3) PMid:20646756
- Abdul KS, Jayasinghe SS, Chandana EP, Jayasumana C, De Silva PM. Arsenic and human health effects: A review. *Environ Toxicol Pharmacol.* 2015; 40:828-46. <https://doi.org/10.1016/j.etap.2015.09.016> PMid:26476885
- Karagas MR, Tosteson TD, Blum J, Morris JS, Baron JA, Klaue B. Design of an epidemiologic study of drinking water arsenic exposure and skin and bladder cancer risk in a U.S. population. *Environ Health Perspect.* 1998; 106:1047-50. <https://doi.org/10.1289/ehp.98106s41047> PMid:9703491 PMcid:PMC1533320
- Carlin DJ, Naujokas MF, Bradham KD, Cowden J, Heacock M, Henry HF, et al. Arsenic and environmental health: State of the science and future research opportunities. *Environ Health Perspect.* 2016; 124:890-9. <https://doi.org/10.1289/ehp.1510209> PMid:26587579 PMCid:PMC4937867
- Seow WJ, Pan WC, Kile ML, Baccarelli AA, Quamruzzaman Q, Rahman M, et al. Arsenic reduction in drinking water and improvement in skin lesions: A follow-up study in Bangladesh. *Environ Health Perspect.* 2012; 120(12):1733-38. <https://doi.org/10.1289/ehp.1205381> PMid:23060367 PMCid:PMC3548283
- Wang W, Wang Q, Zou Z, Zheng F, Zhang A. Human arsenic exposure and lung function impairment in coal-burning areas in Guizhou, China. *Ecotoxic Environ Saf.* 2020; 190:110174. <https://doi.org/10.1016/j.ecoenv.2020.110174> PMid:31927192
- Zeng Q, Zou Z, Wang Q, Sun B, Liu Y, Liang B, et al. Association and risk of five miRNAs with arsenic-induced multiorgan damage. *Sci Total Environ.* 2019; 680:1-9. <https://doi.org/10.1016/j.scitotenv.2019.05.042> PMid:31085440
- Saint-Jacques N, Brown P, Nauta L, Boxall J, Parker L, Dummer TJB. Estimating the risk of bladder and kidney cancer from exposure to low-levels of arsenic in drinking water, Nova Scotia, Canada. *Environ Int.* 2018; 110:95-104. <https://doi.org/10.1016/j.envint.2017.10.014> PMid:29089168
- Pichler G, Grau-Perez M, Tellez-Plaza M, Umans J, Best L, Cole S, et al. Association of arsenic exposure with cardiac geometry and left ventricular function in young adults. *Circ Cardiovasc Imaging.* 2019; 12(5):e009018. <https://doi.org/10.1161/CIRCIMAGING.119.009018> PMid:31060373 PMCid:PMC6668025
- Dangleben NL, Skibola CF, Smith MT. Arsenic immunotoxicity: A review. *Environ Health.* 2013; 12(1):73. <https://doi.org/10.1186/1476-069X-12-73> PMid:24004508 PMCid:PMC3848751
- Sodhi KK, Kumar M, Agrawal PK, Singh DK. Perspectives on arsenic toxicity, carcinogenicity and its systemic remediation strategies. *Environ Technol Innov.* 2019; 16(1):100462. <https://doi.org/10.1016/j.jeti.2019.100462>
- Aposhian HV, Aposhian MM. Newer developments in arsenic toxicity. *J Am Coll Toxicol.* 1989; 8:1297-305. <https://doi.org/10.3109/10915818909009121>
- Ratnaike RN. Acute and chronic arsenic toxicity. *Postgraduate Med J.* 2003; 79:391-6. <https://doi.org/10.1136/pmj.79.933.391> PMid:12897217 PMCid:PMC1742758
- Jomova K, Jenisova Z, Feszterova M, Baros S, Liska J, Hudecova D, et al. Arsenic: Toxicity, oxidative stress and human disease. *J Appl Toxicol.* 2011; 31:95-107. <https://doi.org/10.1002/jat.1649> PMid:21321970
- Watanabe T, Hirano S. Metabolism of arsenic and its toxicological relevance. *Arch Toxicol.* 2013; 87:969-79. <https://doi.org/10.1007/s00204-012-0904-5> PMid:22811022
- Lindberg AL, Kumar R, Goessler W, Thirumaran R, Gurzau E, Koppova K, et al. Metabolism of low-dose inorganic arsenic in a central European population: Influence of sex and genetic polymorphisms. *Environ Health Perspect.* 2007; 115:1081-6. <https://doi.org/10.1289/ehp.10026> PMid:17637926 PMCid:PMC1913583
- Mittal M, Flora SJ. Vitamine E supplementation protects oxidative stress during arsenic and fluoride antagonism in male mice. *Drug Chem Toxicol.* 2007; 30:263-81. <https://doi.org/10.1080/01480540701380075> PMid:17613011
- Liu J, Liv Y, Goyer RA, Achanzar W, Waalkes MP. Metallothionein-I/II null mice are more sensitive than wild-type mice to the hepatotoxic and nephrotoxic effects of chronic oral or injected inorganic arsenicals. *Toxicol Sci.* 2000; 55:460-7. <https://doi.org/10.1093/toxsci/55.2.460> PMid:10828279
- Ramirez P, DelRazo LM, Gutierrez-Ruiz MC, Gonsebatt ME. Arsenite induces DNA-protein crosslinks and cytokeratin expression in the

WRL-68 human hepatic cell line. *Carcinogenesis*. 2000; 21:701-6. <https://doi.org/10.1093/carcin/21.4.701> PMid:10753206

20. Hu Y, Li J, Lou B, Wu R, Wang G, Lu C, et al. The role of reactive oxygen species in arsenic toxicity. *Biomolecules*. 2020; 10(2):240. <https://doi.org/10.3390/biom10020240> PMid:32033297 PMCid:PMC7072296

21. Silva CS, Kudlyk T, Tryndyak VP, Twaddle NC, Robinson B, Gu Q, et al. Gene expression analyses reveal potential mechanism of inorganic arsenic-induced apoptosis in zebrafish. *J Appl Toxicol*. 2023; 43(12):1872-82. <https://doi.org/10.1002/jat.4520> PMid:37501093

22. Pace C, Dagda R, Angenmann J. Antioxidants protect against arsenic induced mitochondrial cardio-toxicity. *Toxics*. 2017; 5(4):38. <https://doi.org/10.3390/toxics5040038> PMid:29206204 PMCid:PMC5750566

23. Shabir I, Pandey VK, Shams R, Dar AH, Dash KK, Khan SA, et al. Promising bioactive properties of quercetin for potential food applications and health benefits: A review. *Front Nutr*. 2022; 9:999752. <https://doi.org/10.3389/fnut.2022.999752> PMid:36532555 PMCid:PMC9748429

24. Liu Z, Ren Z, Zhang J, Chuang CC, Kandaswamy E, Zhou T, et al. Role of ROS and nutritional antioxidants in human diseases. *Front Physiol*. 2018; 9:477. <https://doi.org/10.3389/fphys.2018.00477> PMid:29867535 PMCid:PMC5966868

25. Das N, Bachhawat BK, Mahato SB, Basu MK. Plant glycosides in liposomal drug delivery system. *Biochem J*. 1987; 247:359-61. <https://doi.org/10.1042/bj2470359> PMid:3426542 PMCid:PMC1148416

26. Jiang Q, Yin J, Chen J, Ma X, Wu M, Liu G, et al. Mitochondria targeted antioxidants: A step towards disease treatment. *Oxid Med Cell Longev*. 2020; 2020:8837893. <https://doi.org/10.1155/2020/8837893> PMid:33354280 PMCid:PMC7735836

27. Purohit D, Jalwal P, Manchanda D, Saini S, Verma R, Kaushik D, et al. Nanocapsules: An emerging drug delivery system. *Recent Pat Nanotechnol*. 2023; 17(3):190-207. <https://doi.org/10.2174/187221051666220210113256> PMid:35142273

28. Hoff J, Rlatg LVT. Methods of blood collection in the mouse. *Lab Anim*. 2000; 29(10):47-53.

29. Tyagi R, Lala S, Verma AK, Nandy AK, Mahato SB, Maitra A, et al. Targeted delivery of arjunglucoside 1 using surface hydrophilic and hydrophobic nanocarriers to combat experimental leishmaniasis. *J Drug Target*. 2005; 13:161-71. <https://doi.org/10.1080/10611860500046732> PMid:16036304

30. Karim S, Bhandari U, Kumar H, Salam A, Siddiqui MAA, Pillai KK. Doxorubicin induced cardiotoxicity and its modulation by drugs. *Ind J Pharm*. 2001; 33:203-7.

31. Beyer JWF, Fridovich I. Assaying for superoxide dismutase activity: Some large consequences of minor changes in conditions. *Anal Biochem*. 1987; 161(2):559-66. [https://doi.org/10.1016/0003-2697\(87\)90489-1](https://doi.org/10.1016/0003-2697(87)90489-1) PMid:3034103

32. Mandal AK, Das S, Mitra M, Chakrabarti RN, Chatterjee M, Das N. Vesicular flavonoid in combating diethylnitrosamine induced hepatocarcinoma in rat mode. *J Exp Ther Oncol*. 2008; 7:123-33.

33. Moragon AC, DeLucas GN, Encarnacion LFM, Rodriguez MAS, Jimenez FJA. Antioxidant enzymes, occupational stress and burnout in workers of a prehospitalary emergency service. *Eur J Emerg Med*. 2005; 12:111-15.

34. Sarkar S, Das N. Mannosylated liposomal flavonoid in combating age-related ischemic-reperfusion induced oxidative damage in rat brain. *Mech Ageing Dev*. 2006; 127:391-97. <https://doi.org/10.1016/j.mad.2005.12.010> PMid:16480758

35. Castro VM, Soderstrom M, Carlberg I, Widersten M, Platz A, Mannervik B. Differences among human tumor cell lines in the expression of glutathione transferases and other glutathione-linked enzymes. *Carcinogenesis*. 1990; 11:1569-76. <https://doi.org/10.1093/carcin/11.9.1569> PMid:2401046

36. Maiti S, Chatterjee AK. Differential response of cellular antioxidant mechanism of liver and kidney to arsenic exposure and its relation to dietary protein deficiency. *Environ Toxicol Pharmacol*. 2000; 8:227-35. [https://doi.org/10.1016/S1382-6689\(00\)00046-6](https://doi.org/10.1016/S1382-6689(00)00046-6) PMid:10996542

37. Mandal AK, Das N. Sugar coated liposomal flavonoid: A unique formulation in combating carbon tetrachloride induced hepatic oxidative damage. *J Drug Target*. 2005; 13:305-15. <https://doi.org/10.1080/10611860500230278> PMid:16199374

38. Betainder C, Fontaine E, Keriel C, Leuerve XM. Determination of mitochondrial oxygen species: Methodological aspects. *J Cell Mol Med*. 2002; 6:175-87. <https://doi.org/10.1111/j.1582-4934.2002.tb00185.x> PMid:12169203 PMCid:PMC6740075

39. Mandal AK, Sinha J, Mandal S, Mukhopadhyay S, Das N. Targeting of liposomal flavonoid to liver in combating hepatocellular oxidative damage. *Drug Deliv*. 2002; 9:181-85. <https://doi.org/10.1080/15227950290097615> PMid:12396735

40. Lowry OH, Rosebrough NJ, Farr AL, Randall RG. Protein measurement with Folin Phenol reagent. *J Biol Chem*. 1951; 193:265-77. [https://doi.org/10.1016/S0021-9258\(19\)52451-6](https://doi.org/10.1016/S0021-9258(19)52451-6) PMid:14907713

41. Sarkar S, Mandal S, Sinha J, Mukhopadhyay S, Das N, Basu MK. Quercetin: Critical evaluation as an anti leishmanial agent in vivo in hamsters using different vesicular delivery modes. *J Drug Target*. 2002; 10:573-78. <https://doi.org/10.1080/106118021000072681> PMid:12683660

42. Guha Mazumder DN, De BK, Santra A, Ghosh N, Das S, Lahiri S, et al. Randomized placebo-controlled trial of 2,3-dimercapto-1-propanesulfonate (DMPS) in therapy of chronic arsenicosis due to drinking arsenic-contaminated water. *Clin Toxicol*. 2001; 39:665-74. <https://doi.org/10.1081/CLT-100108507> PMid:11778664

43. Li L, Lei X, Chen L, Ma Y, Luo J, Liu X, et al. Protective mechanism of quercetin compounds against acrylamide-induced hepatotoxicity. *Food Sci Human Wellness*. 2024; 13(1):225-40. <https://doi.org/10.26599/FSHW.2022.9250019>

44. Das S, Santra A, Lahiri S, Guha Mazumder DN. Implications of oxidative stress and hepatic cytokine (TNF-alpha and IL-6) mresponse in the pathogenesis of hepatic collagenesis in chronic arsenic toxicity. *Toxicol Appl Pharmacol*. 2005; 204:18-26. <https://doi.org/10.1016/j.taap.2004.08.010> PMid:15781290

45. Aherne SA, Brien'O NM. Mechanism of protection by the flavonoids, quercetin and rutin, against tert-butylhydroperoxide- and menadione-induced DNA single strand breaks in Caco-2 cells. *Free Radic Biol Med*. 2000; 29(6):507-14. [https://doi.org/10.1016/S0891-5849\(00\)00360-9](https://doi.org/10.1016/S0891-5849(00)00360-9) PMid:11025194

46. Roeb E. Matrix metalloproteinases and liver fibrosis (translational aspects). *Matrix Biol*. 2018; 68-69:463-73. <https://doi.org/10.1016/j.matbio.2017.12.012> PMid:29289644